POLITECNICO DI TORINO
Repository ISTITUZIONALE

Numerical and experimental evaluation of SLA polymers adhesion for innovative bio-MEMS

(Article begins on next page)

24 April 2024

BioM&M_2018

Numerical and experimental evaluation of SLA polymers adhesion for innovative bio-MEMS

Giorgio De Pasquale[a],*, Lorena Zappulla[a], Luciano Scaltrito[b], Valentina Bertana[b]

aDepartment of Mechanical and Aerospace Engineering, Politecnico di Torino, 10129, Italy
bDepartment of Applied Science and Technology, Politecnico di Torino, 10129, Italy

Abstract

Polymer stereolithography is well known additive process already used in bio-MEMS and labs-on-chip applications. The same polymerization process is used in this paper to replace traditional adhesives and to provide fast, reliable and transparent joint with different materials as PMMA in microfluidic devices. The properties of adhesion between resin and transparent covering layers are characterized with mechanical peeling tests which are also used to validate numerical models based on cohesive approach. The influence of process parameters on mechanical properties of the joint are also analyzed.

Keywords: MEMS; labs-on-chip; peeling tests; adhesives; microfluidics.

1. Introduction

Microfluidics applied to biotechnology is attracting the interest of research activities related to scientific and industrial applications. In particular, microfluidic systems as labs-on-chip and bio-MEMS based on polymers are characterized by high performances and low cost. They are hybrid devices that integrate fluidic and electronic

---

* Corresponding author. Tel.: +39-011-0906912; fax: +39-011-0906999.
E-mail address: giorgio.depasquale@polito.it

components on the same chip with the aim of reducing chemical and biological laboratories to a microscale system [1]. The main application fields of 3D-printed labs-on-chip are bioengineering, medicine, biology and optoelectronics [2]. In the last decades, microfluidic devices have been used for the recognition of potential chemical and bacteriological threats and for DNA sequencing [3, 4]. Besides consolidated fabrication technologies as soft-lithography, embossing, and laser ablation [5], the recent adoption of additive manufacturing methods is opening to process simplification, time to market reduction and costs minimization [6].

The 3D printing of bio-MEMS involves the fabrication process and specific design issues. The most consolidated additive processes are stereolithography (SLA), laser ablation and fused deposition modeling (FDM), while some other methods as electron beam melting (EBM) and bioprinting are under investigation. With SLA, the liquid resin is exposed to UV light or laser and the component is created layer-by-layer. This process is relatively simple and fast but it is limited to few materials and is accompanied by roughness of surfaces. In the recent past, labs-on-chip where fabricated with glass and silicon which requires long processes with several steps and limitations in building complicated 3D shapes. Again, polymers are preferred due to specific properties of transparency and biocompatibility. Polymers used in bio-MEMS are generally of three typologies: a) photosensitive resins used for SLA or lithography, b) thermoplastic polymers as PMMA processed at the glass transition temperature, c) elastomers characterized by high elasticity and permeability to CO_2 and O_2 suitable for contacting cells.

Numerical modeling of structural-fluidic coupled systems and computational fluid dynamics (CFD) approaches are used in the design stage. About experimental testing of prototypes, labs-on-chip are validated under pressure to verify the sealing of internal channels and chambers. The device is filled with incompressible fluid under increasing pressure with obstructed outlet until the explosion. The test provides also the maximum operative pressure of the device. Optical characterizations and detections are also used to check printing issues and validation of transparency. Another characterization procedure, applied in this paper, is based on the peeling tests, which determines the adhesion strength between different substrates. The peeling tests may have different configurations of force-substrate angular orientations. Several peeling modes were presented in literature. In 1944, Rivlin [7] described the peeling process between surfaces by means of adhesion energy associated to the transverse section of the coupled system. This first tentative model has been improved by the introduction of several parameters associated to the viscoelasticity of the peeling process and the differences among loading conditions and temperature. In 1971, Kendall [8] introduced in the model the surface energy and the peeling angle. Then Pesika et al. [9] described the critical peeling angle to distinguish two different regimes of the process: when the actual angle is lower than the critical value, the peeling force is independent to the same peeling angle, otherwise the force increases with angle decreasing. With Brown et al. [10], the peeling velocity has been included in the modeling to estimate the strain energy of the process. The dependency between the cohesive strength and peeling velocity was analyzed by Choi et al. [11], while other models relate the peeling force to the friction and eventual pre-stress state inside the adhesive surface. Tian et al. [12] considered the peeling force as the composition of normal force of adhesion and lateral friction force. More recently, in 2009, Chen et al. [13] calculated that the press-stress state inside the adhesive surface is able to increase significantly the peeling force, with great benefits on the joined surface, only for small peeling angles. Lamblet et al. [14] discussed the adhesion between heterogeneous surfaces; other relevant researches have been conducted by Chen et al. [15] and Huang et al. [16].

In this paper, the fabrication process of lab-on-chip based on SLA additive method is investigated. In particular, the SLA process is used to join together the substrate layer made of polymerized resin grown layer-by-layer and the PMMA transparent cover. Compared to traditional processes, the two materials are not coupled by using adhesives (requiring additional materials, transparency issues and dedicated step of the fabrication) by using the polymerization of the same resin as adherent media. Then, the peeling test method is used to validate the adhesion strength of the joint with different treatments of surface and mechanical manipulations of the resin. Finally, numerical model of adhesion is calibrated with the experimental parameters derived from the peeling tests able to support the calculation of cohesion limit in different geometries.

2. SLA samples

Labs-on-chip samples fabricated with resin polymerization by SLA and PMMA are fabricated with different surface treatments and mechanical manipulation of the resin. The adhesion force is then measured for the different

combinations. The resin used for polymerization process is the FTD-Standard Blend, already characterized by the authors in [17] with reference to the mechanical properties related to the SLA process parameters. The resin has good wettability (90° contact angle), which facilitate the adhesion to the PMMA cover. After SLA process, samples are glued on a metal support to facilitate the installation on the tensile machine used for the next peeling tests. The two configurations of resin re-coater reported in Fig. 1 are used: manual movement within lateral rails (a) and automatic motorization through tooted belts (b)
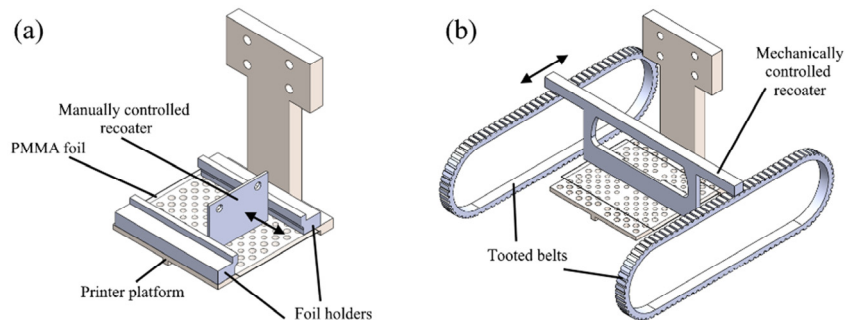

Fig. 1. Resin re-coater in double configurations: manual (a) and automatic (b).

2.1. SLA with manual re-coater

In the first sample set, the resin is adjusted by manual re-coater layer-by-layer before the laser activation. The PMMA (not treated) with size 35x10 mm is adjusted on the SLA machine stage. Four layers of resin are deposited and polymerized on the PMMA, with 100 µm thickness each. The polymerization is obtained with 405 nm laser at 10 mW power, double hatching at 45° and 135°, inner scanning speed 800 mm/s and contour scanning speed 1500 mm/s. After polymerization, the samples are washed with isopropanol to remove the residues of the liquid resin. The polymerization is then completed with 10 min post-curing in UV oven. The sample at the end of the process is represented in Fig. 2.

In the second set of samples, the PMMA cover is treated with ethanol for 10 min before to start the polymerization. The treatment has the goal to remove possible impurities on the PMMA surface.

2.2. SLA with automatic re-coater

In the third samples set, automatic resin re-coater is used to improve to uniformity of the liquid layer before laser activation. The resin polymerization through SLA process is conducted with the same process parameters mentioned before. The PMMA cover has been treated with O_2 plasma with 60% oxygen percentage, 0.3 kW power and 10 min exposure time. After the plasma treatment, three layers of resin with 100 µm thickness are polymerized on it. The isopropanol washing and post-curing process are repeated as before.

Fig. 2. Sample composed by SLA polymerized resin and PMMA cover.

3. Peeling tests: setup and results

The peeling tests are performed with the standard electro-mechanical tensile testing machine MTS Q Test 10 (10 kN max capacity, 1016 mm max travel). The peeling angle used for samples characterization is 30°, the displacement control mode with 5 mm/min velocity is applied, and 500 N load cell is used. The results of peeling tests are reported in the force-displacement curves of Fig. 3 and the tests setup configuration is reported in Fig. 4.
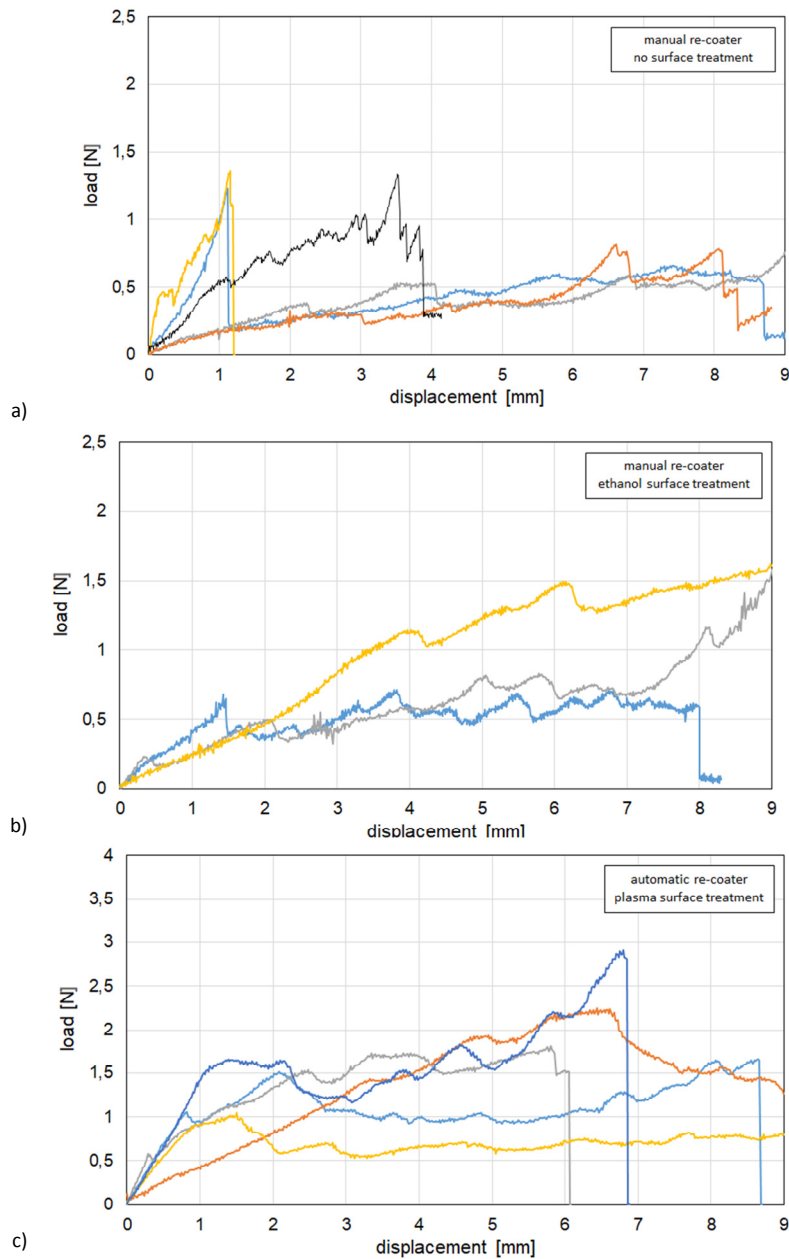

a)

b)

c)

Fig. 3. Results of peeling tests with manual re-coater without surface treatment (a) and with ethanol treatment (b), and with automatic re-coater and plasma surface treatment (c).
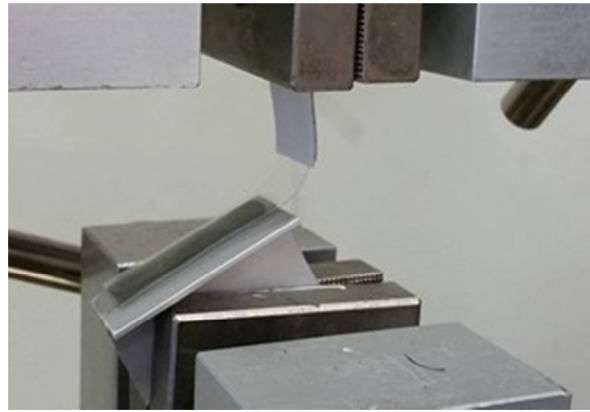
Fig. 4. Peeling test at 30° and 5 mm/min velocity.

4. Numerical modeling

The adhesion between resin and PMMA materials is modeled with FEM approach to predict the joint failure under the effect of peeling forces. The cohesive model is calibrated with the parameters obtained from peeling tests described before when the automatic re-coater is used.

The 2D model reported in Fig. 5 includes structural elements for polymerized resin (0.3 mm thickness) and PMMA cover (0.175 mm thickness), with mesh size of 0.05 mm and 0.01 mm in the region of materials separation. The interface between materials is modeled with the "cohesive zone material" approach [18]: the cohesive force between the two surfaces is described with exponential curve or, in the simplified version, with bilinear curve [19]. The force threshold causing the separation of contact surfaces is related to the inter-laminar energy of fracture that depends to the parameters imposed to the force-displacement curve [20]. The material properties considered in the model are E = 2100 MPa and ν = 0.38 for PMMA and E = 5500 MPa and ν = 0.3 for the polymerized resin.
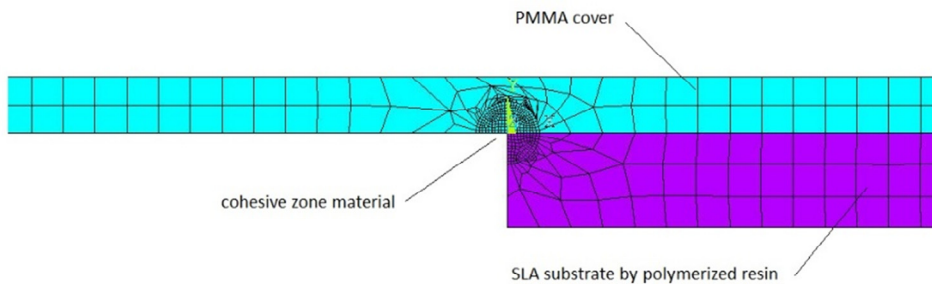

Fig. 5. FE model of cohesive zone between polymerized resin and PMMA.

The exponential model requires empirical parameters, which are derived from peeling tests. The maximum stress at interface is obtained from Fig. 3c: the linear elastic part of each curve is used to determine the maximum force applicable to the first front of the joint before local adhesion failure. This force is divided by unit area (given by sample width and mesh size in the direction orthogonal to peeling). The stress obtained has been corrected with the standard deviation of experimental results, giving finally σ_{max} = 3.6 MPa. The displacement corresponding to the first front detachment in normal direction is obtained by the average values of the same curves, at the end of linear response, giving δ_n^c = 1.25 mm. The displacement in tangent direction is considered $\delta_t^c = \delta_n^c$ as first approximation, as already documented in previous works [21]. The result of numerical model provided the maximum interface displacement δ_n^{max} = 1.89 mm that is in agreement with experimental measurements in the condition of detachment of the first front of the joint.

5. Discussions and conclusions

Samples polymerized with manual re-coater in the SLA machine reveals large variability in the force-displacement curves of peeling tests. In particular, among samples without any treatment, two of them show the force peak at 1.3 N followed by sudden failure; instead, in the other cases, samples present almost constant force plateau at lower levels (0.5 – 0.7 N). Samples with ethanol treatment on the PMMA surface reveals unpredictable trends of force-displacement, with two samples that failed instantaneously at the beginning of force application (not reported in the graphs).

Samples fabricated with automatic re-coater instead reveal more stable behavior; here the peeling force is almost constant for each sample during the entire detachment of materials with values in the range 0.5 – 2 N. However, the variability among the peeling forces of the samples is still large. The uniformity of the liquid resin layer deposited is responsible of the regularity of peeling force during the test. The automatic re-coater is then effective to improve the adhesion quality and peeling force prediction.

The numerical model developed, based on the cohesive zone material, is able to predict with reasonable accuracy the first failure of adhesive detachment by comparing the normal displacement between surfaces. The model can be used by iterative approach to calculate the failure of resin-PMMA joints under increasing values of the applied load.

References

[1]   A.T. Giannitsis, Estonian Journal of Engineering 17 (2011) 109.
[2]   D. Psaltis, S. Quake, C. Yang, Nature 442 (2006) 381-386.
[3]   D. Breslauer, P. Lee, L. Lee, Molecular BioSystems 2 (2006) 97-112.
[4]   D. Beebe, G. Mensing, G. Walker, Annual Review Biomedical Engineering 4 (2002) 261-86.
[5]   H. Klank, J.P. Kutter, O. Geschke, Lab Chip 2 (2002) 242-247.
[6]   C.M. Ho, S.H. Ng, K.H. Li, Y.J. Yoon, Lab Chip 15 (2015) 3627-3637.
[7]   R. Rivlin, Paint Technol. 9 (1944) 215.
[8]   K. Kendall, J. Phys. D Appl. Phys. 4 (1971) 1186.
[9]   N.S. Pesika, Y. Tian, B.X. Zhao, K. Rosenberg, H.B. Zeng, P. McGuiggan, K. Autumn, J.N. Israelachvili, J. Adhesion 83 (2007) 383.
[10]   H.R. Brown, Annu. Rev. Mater. Sci. 21 (1991) 463.
[11]   S.T. Choi, S.R. Lee, Y.Y. Earmme, J. Phys. D Appl. Phys. 41 (2008) 074023.
[12]   Y. Tian, N. Pesika, H.B. Zeng, K. Rosenberg, B.X. Zhao, P. McGuiggan, K. Autumn, J. Israelachvili, Proc. Natl. Acad. Sci., USA, 103 (2006) 19320.
[13]   B. Chen, P.D. Wu, H.J. Gao, J. R. Soc. Interface 6 (2009) 529.
[14]   M. Lamblet, E. Verneuil, T. Vilmin, A. Buguin, P. Silberzan, L. Leger, Langmuir 23(2007) 6966.
[15]   H. Chen, X. Feng, Y. Huang, Y.G. Huang, J.A. Rogers, J. Mech. Phys. Solids 61 (2013) 1737.
[16]   Y.G. Huang, W.X. Zhou, K.J. Hsia, E. Menard, J.U. Park, J.A. Rogers, A.G. Alleyne, Langmuir 21 (2005) 8058.
[17]   G. De Pasquale, V. Bertana, L. Scaltrito, Microsyst. Technol. (2018)
[18]   K.C. Gopalakrishnan, R. Ramesh Kumar, S. Anil Lal, J. Sandw. Struct. Mater. 14 (2012) 679–93.
[19]   A. Needleman, Int. J. Fract. 42 (1990) 21-40.
[20]   A. Needleman, J. Appl. Mech. 54 (1987) 525-531.
[21]   H.S. Waseem, K. Kumar, SSRG Int. J. Mech. Eng. 1 (2014).